PCCP

Accepted Manuscript

This article can be cited before page numbers have been issued, to do this please use: E. Lucenti, E. Cariati, X. Liu, Y. Geng, A. Forni, S. Righetto, S. Decurtins and S. Liu, *Phys. Chem. Chem. Phys.*, 2017, DOI: 10.1039/C7CP04687A.

ROYAL SOCIETY OF CHEMISTRY

rsc.li/pccp

View Article Online
DOI: 10.1039/C7CP04687A

Journal Name

ARTICLE

Stimuli-Responsive NLO Properties of Tetrathiafulvalene-Fused Donor–Acceptor Chromophores

Received 00th January 20xx,
Accepted 00th January 20xx

DOI: 10.1039/x0xx00000x

www.rsc.org/

E. Cariati,[a,b] X. Liu,[c] Y. Geng,[c] A. Forni,[b] E. Lucenti,*[,b] S. Righetto,[a] S. Decurtins[c] and S.-X. Liu*[,c]

The second-order nonlinear optical (NLO) properties of two tetrathiafulvalene (TTF)-fused electron donor–acceptor dyads have been determined by Electric Field Induced Second Harmonic generation (EFISH) technique and theoretically rationalized. Dyads TTF-dppz (**1**) and TTF-BTD (**2**) were obtained by direct fusion of a TTF electron donor unit either with a dipyrido[3,2-*a*:2′,3′-*c*]phenazine (dppz) or a benzothiadiazole (BTD) electron acceptor moiety. The dyad **1** acts as a reversible acido-triggered NLO switch by protonation/deprotonation at two nitrogen atoms of the dppz acceptor moiety induced by sequential exposure to HCl and ammonia vapors (enhancement factor equal to 2). Dyad **2**, on the other hand, displays redox-tunable NLO properties upon two consecutive oxidations to its radical cation $\mathbf{2}^{+\cdot}$ and dication $\mathbf{2}^{2+}$ species. The formation of the radical cation $\mathbf{2}^{+\cdot}$ is accompanied by a high NLO response (enhancement factor equal to 2.6) and inversion of the sign of $\mu\beta_\lambda$ associated with a redistribution of the frontier molecular orbitals compared to that of its neutral species. The dication $\mathbf{2}^{2+}$ exhibits a negative and lower $\mu\beta_\lambda$, due to a completely inverted distribution of the frontier molecular orbitals with respect to those of its neutral species, leading to a scarcely polar species in the excited state.

Introduction

Tetrathiafulvalene (TTF) and its derivatives have been intensively investigated, as strong electron donors, for their potential applications, which include single-component molecular conductors and electrochemical switches,[1] chemical sensors,[2] photovoltaic devices,[3] and organic field-effect transistors (OFETs).[4] They have also been studied as active chromophores for second order nonlinear optics (NLO), an appealing property for preparation of materials for optical communications, signal processing, data storage and electro-optical devices.[5] In particular, the possibility of switching "on and off" the second order NLO response both at molecular and macroscopic level by external stimuli has received increasing attention.[6] Typically the switching can be achieved by applying different stimuli spanning from redox or electrochemical reactions to protonation/deprotonation processes or photoexcitation.[7] Within this context, the TTF unit, with its characteristic three stable redox states (TTF, the radical cation $TTF^{+\cdot}$, and the dication TTF^{2+}) represents a versatile and still rather unexplored tecton for the development of NLO materials and switches.

The first report on the second order NLO properties of a TTF derivative, designed according to the push-pull strategy by covalent linkage of the electron donor TTF to electron acceptor groups through ethylenic spacers, appeared 20 years ago.[8a] Since then, much effort has been devoted to enhance the NLO response of the resulting molecular systems by increasing the electron donor (D)/acceptor (A) strength and the length of the π-conjugated spacers.[8-9] Such strategies for the optimization of the second harmonic generation (SHG) signal were also supported by density functional theory (DFT) calculations, which have been applied to rationalize the NLO behaviour of various TTF-based molecules.[10] In one of these theoretical studies, Muhammad put emphasis on TTF-fused phenazine systems.[10h] Importantly, TTF-fused D-A systems achieved by the annulation of TTF with heteroatom-containing A moieties display desirable features such as pronounced and energetically low-lying intramolecular charge-transfer (ICT) transitions and high polarizability, that make them excellent candidates for NLO applications.[11] However, to the best of our knowledge, their NLO response has never been experimentally investigated.

As a consequence, we turned our attention to explore stimuli-responsive NLO properties of dyads TTF-dppz (**1**) and TTF-BTD (**2**) obtained by direct fusion of a TTF unit either with dipyrido[3,2-*a*:2′,3′-*c*]phenazine (dppz)[12] or with a benzothiadiazole (BTD)[13] core (Figure 1). Herein we demonstrate both experimentally and theoretically that **1** acts as a reversible acido-triggered NLO switch by sequential exposure to HCl and ammonia vapors, while **2** exhibits a redox-tunable NLO response through sequential chemical oxidations to its radical cation $\mathbf{2}^{+\cdot}$ and dication $\mathbf{2}^{2+}$, respectively.

[a] *Department of Chemistry, Università degli Studi di Milano, via Golgi 19, 20133 Milano, and INSTM UdR of Milano, Italy*
[b] *ISTM-CNR, Institute of Molecular Science and Technologies of CNR, via Golgi 19, 20133 Milano, and INSTM UdR of Milano, Italy*
[c] *Department of Chemistry and Biochemistry, University of Bern, Freiestrasse 3, CH-3012 Bern, Switzerland*

†Electronic Supplementary Information (ESI) available: Figure S1 (^{1}H COSY of **1**); Figure S2 (^{1}H COSY of **1**·$(HCl)_2$); Figure S3 (optimized molecular structure of **1** and **2**); Table S1 (computational details on all the possible protonated forms of **1**). See DOI: 10.1039/x0xx00000x

View Article Online
DOI: 10.1039/C7CP04687A

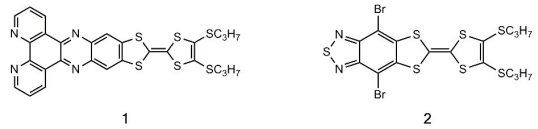

Figure 1. Molecular structures of TTF-dppz (**1**) and TTF-BTD (**2**).

Experimental

General Comments

Optical absorption spectra were recorded on a Perkin Elmer Lambda 25 UV/vis spectrometer. ^{1}H NMR and ^{1}H-^{1}H COSY spectra were recorded on a Bruker AVANCE-400 instrument (400 MHz). Chemical shifts are reported in parts per million (ppm) and are referenced to the residual solvent peak (CD_2Cl_2, ^{1}H 5.35 ppm). Coupling constants (*J*) are given in hertz (Hz) and are quoted to the nearest 0.5 Hz. Peak multiplicities are described in the following way: s, singlet; d, doublet; t, triplet; m, multiplet; br, broad peak. NLO switches *via* protonation/deprotonation in solution are commonly studied by the HRS technique since EFISH measurements are usually considered off limits for ionic species. However, the suitability of the EFISH technique for such studies has recently been reported when working with a solvent of low dielectric constant, such as $CHCl_3$, which favors ion pairing.[14] EFISH measurements were carried out in $CHCl_3$ (treated with basic Al_2O_3 and degassed for 30 minutes under a nitrogen stream before use) with an incident wavelength of 1907 nm, obtained by Raman-shifting the fundamental 1064 nm wavelength produced by a Q-switched, mode-locked Nd^{3+}:YAG laser manufactured by Atalaser. The $\mu\beta_\lambda$ values reported are the mean values of 4 measurements performed on the same sample.

Synthesis and Characterization.

Compounds **1**[12] and **2**[13] were prepared according to literature procedures. Protonation of **1**: a 2×10^{-4} M solution of **1** in $CHCl_3$ (6.1 mg in 50 mL) was exposed to HCl vapor for 30 minutes. The colour changed from purple to blue. A ^{1}H NMR study to elucidate which nitrogen atoms undergo protonation was performed on a 1.75 M solution of **1** (0.8 mg) in CD_2Cl_2 (0.75 mL). ^{1}H NMR data for **1** (400 MHz, CD_2Cl_2): δ = 9.62–9.64 (d, *J* = 9 Hz, 2H), 9.30–9.31 (d, *J* = 4.5 Hz, 2H), 8.18 (s, 2 H), 7.87–7.90 (m, 2H), 2.87–2.91 (t, 4H), 1.68–1.78 (m, 4 H), 1.05–1.09 (t, 6H) ppm. ^{1}H NMR data for the protonated form (400 MHz, CD_2Cl_2): δ = 9.96–9.94 (d, *J* = 6 Hz, 2H), 9.63 (br, 2H), 8.24 (br, 4H) ppm (the signals for the protons of propyl moieties are hardly discernible due to strong and broad peaks at δ 5.35 and 1.71 ppm associated with aqueous HCl). On the basis of ^{1}H NMR spectra, the downfield shifts of all protons of the phenanthroline moiety are consistent with protonation of the two N atoms on the pyridyl subunit. The signals of **1** are restored after exposure to NH_3 vapor.

Oxidation of **2** to radical cation $\mathbf{2}^{+\cdot}$: To a 8×10^{-4} M solution of **2** in $CHCl_3$ (12.5 mg in 25 mL) were added 2 equivalents of $NOBF_4$ (265 μL of a 0.15 M solution in CH_3CN). The reaction was kept under nitrogen. Oxidation of **2** to the dication $\mathbf{2}^{2+}$: to a 1×10^{-3} M solution of **2** in $CHCl_3$ (15.9 mg in 25 mL) were added 3 equivalents of $NOBF_4$ (550 μL of a 0.14 M solution in CH_3CN).

Computational Details.

The molecular structures of all compounds have been optimized *in vacuo* within the DFT approach, using the PBE0 functional,[15-16] which has previously been judged as well suited for describing the electronic features of a series of organic dyes.[17] Geometry optimizations have been performed starting from the related X-ray molecular structures reported in refs. 12a and 13. In the case of the oxidized forms of **2**, twisted starting geometries have also been tested to explore the full potential energy surfaces of these species. The 6-311^{++}G(d,p) basis set was chosen for all atoms. Standard vertical Time Dependent DFT (TDDFT) calculations[18-20] have been carried out at the TD-PBE0/6-311++G(d,p) level using the so-called non-equilibrium approach, to determine the absorption wavelengths. The same functional has been previously adopted for evaluating absorption energies of analogue TTF-fused phenazine systems.[10h] Moreover, the CAM-B3LYP functional[21] was tested for TDDFT calculations on **1** and **2** but provided strongly underestimated absorption wavelengths, even including solvent effects through standard PCM approaches. Hyperpolarizabilities have been computed at the same frequency as used in the experiment, using the Coupled Perturbed Kohn Sham (CPKS) approach with the CAM-B3LYP functional, which was recently recommended for hyperpolarizability calculations of mid-size organic chromophores.[22] All calculations have been performed with the Gaussian suite of programs.[23]

Results and Discussion

As illustrated in Figure 2, **1** exhibits an intense ICT absorption band around 542 nm (18450 cm^{-1}) in $CHCl_3$. This transition is dominated by a one-electron excitation from the HOMO localized on the TTF moiety to the LUMO on the dppz part.[12a] Upon exposure to HCl vapor, the colour of the solution changes from purple to blue and the absorption maximum is red-shifted by 1810 cm^{-1} to 601 nm. This red-shift can be mainly attributed to the lowering of the energy of the LUMO, because protonation is expected to perturb essentially the dppz moiety, increasing its electron acceptor ability. As shown in the ^{1}H NMR spectra (Figure 3), the down-field shifts of all protons of the phenanthroline moiety are indicative of the protonation of two N atoms on the pyridyl subunits, which is consistent with X-ray structures of dppz analogues.[24]

View Article Online
DOI: 10.1039/C7CP04687A

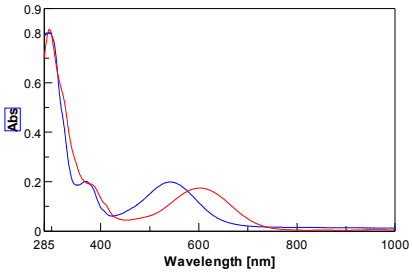

Figure 2. Optical absorption spectra of **1** in $CHCl_3$ (1×10^{-4} M) before (blue) and after (red) exposure to HCl vapor for 20 minutes.

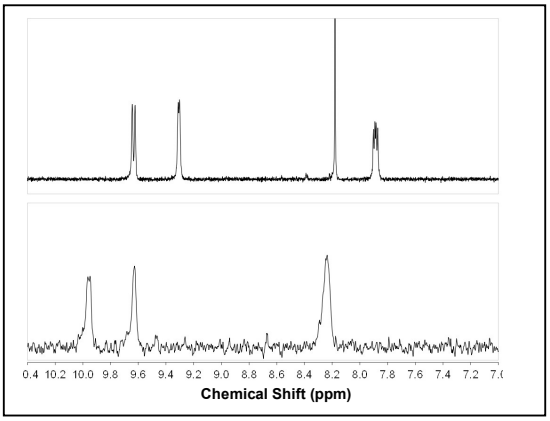

Figure 3. Aromatic region in the ^{1}H NMR of **1** (1.7×10^{-3} M in CD_2Cl_2) before (top) and after (bottom) exposure to HCl vapor for 20 minutes.

The reverse transformation can be induced by treatment of the solution with NH_3 vapor, as confirmed by optical absorption and ^{1}H NMR spectroscopy. This observation prompted us to monitor the second-order NLO properties during a protonation/deprotonation cycle of **1** by the EFISH technique, which provides direct information on the intrinsic molecular NLO properties, through

$$\gamma_{EFISH} = (\mu\beta_{EFISH}/5kT) + \gamma(-2\omega; \omega; \omega; 0)$$

where $\mu\beta_{EFISH}/5kT$ is the dipolar orientational contribution to the molecular nonlinearity, and $\gamma(-2\omega; \omega; \omega; 0)$, the third order polarizability, is a purely electronic cubic contribution to γ_{EFISH} which can usually be neglected when studying the second-order NLO properties of dipolar molecules. Although it has traditionally been used to study neutral molecules, the EFISH technique can be applied to the determination of the second-order NLO response of ionic species by working in a solvent of low dielectric constant like $CHCl_3$, which favours ion-pairing, as previously reported on other organic NLO chromophores.[14]

A positive $\mu\beta_\lambda$ value of **1** in a $CHCl_3$ solution (2×10^{-4} M) was determined to be 370×10^{-48} esu at a 1907 nm non-resonant wavelength (Table 1), in agreement with an increased dipole moment in the electronically excited state (S_1) compared to the ground state (see below).

Table 1. EFISH $\mu\beta_\lambda$, β_λ and β_0 values for compounds **1** and **2**.

Sample	C(M)	$\mu\beta_\lambda$[a]	β_λ[b]	β_0[c]
1	2×10^{-4}	370	106	66
1·(HCl)$_2$	2×10^{-4}	750	81	44
2	10^{-3}	460	136	86
2$^+$	8×10^{-4}	-1200	-142	-27
2^{2+}	10^{-3}	-560	-37	-23

[a] $\mu\beta_\lambda$ $\times10^{-48}$ esu; [b] β_λ $\times10^{-30}$ esu, calculated using computed μ values (see Table 2); [c] Calculated with the two-level model[25].

Upon exposure of the solution of **1** to HCl vapor until complete disappearance of the ICT absorption band at 542 nm, an increase of $\mu\beta_\lambda$ up to 750×10^{-48} esu was observed in agreement with the red-shift of the absorption band caused by an increase of the electron-withdrawing ability of the dppz moiety. Further treatment with NH_3 vapor (after filtration of the solution to remove NH_4Cl, which muddies the solution) restored the original value.

The electronic absorption spectrum of **2** in $CHCl_3$ is given in Figure 4. Similarly to **1**, the intense absorption band at 532 nm (18800 cm^{-1}) corresponds to an ICT transition, which is dominated by a one-electron excitation from HOMO to LUMO, hence from the TTF part to the BTD moiety.[13] It has been demonstrated that **2** can be easily oxidized in solution to its radical cationic species **2$^{+\cdot}$** in the presence of $NOBF_4$.[13] Upon addition of 2 equivalents of $NOBF_4$, the colour of the solution changes from purple to dark green, indicating the formation of **2$^{+\cdot}$**, characterized by a new absorption band at 834 nm (11990 cm^{-1}, Figure 4). This excitation can be attributed to a π-π* transition localized on the $TTF^{+\cdot}$ unit (as supported by theoretical calculations, vide infra). In the attempt to use **2** as a redox-tunable NLO compound, we have measured its EFISH $\mu\beta_\lambda$ response in $CHCl_3$, before and after oxidation with $NOBF_4$. The $\mu\beta_\lambda$ value (Table 1) of **2** is high and positive (460×10^{-48} esu). In contrast, the chemical oxidation leads to an inversion of the sign of $\mu\beta_\lambda$ (-1200×10^{-48} esu) for **2$^{+\cdot}$**.

Further addition of 1 equivalent of $NOBF_4$ to the solution containing **2$^{+\cdot}$**, or direct addition of 3 equivalents of $NOBF_4$ to a solution of **2** in $CHCl_3$, resulted in the formation of the dicationic species **2^{2+}** (Figure 4), as indicated by the colour change from green to pink. EFISH measurements in $CHCl_3$ afforded a $\mu\beta_\lambda$ value of -560×10^{-48} esu (Table 1). This apparent incongruence with an expected further increase of the second order NLO efficiency may be explained with resonance effect at 2ω for **2$^{+\cdot}$**. In fact, a much smaller difference is observed for the corresponding static β_0 (see Table 1).

The molecular structures of **1** and **2** obtained by DFT geometry optimization in the gas phase (see Figure S3) reveal a slightly bent conformation of the conjugated backbone, differently from the solid-state X-ray structures previously reported,[12a,13] where the virtual planarity of the conjugated backbone is dictated most probably by packing forces.

It is worth noting that the concentrations used for EFISH measurements (10^{-3}-10^{-4} M) exclude any occurrence of aggregation forms of the chromophores in solution.

View Article Online
DOI: 10.1039/C7CP04687A

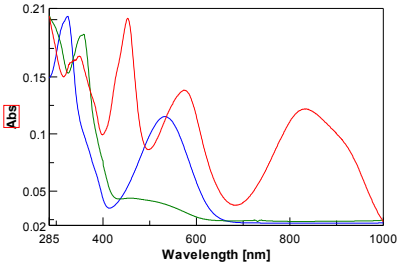

Figure 4. Optical absorption spectra of **2** in $CHCl_3$ solution (1×10^{-4} M) (blue); after addition of 2 eq. of $NOBF_4$ to give $\mathbf{2}^{+\cdot}$(red); after addition of total 3 eq. of $NOBF_4$ to give $\mathbf{2}^{2+}$ (green).

Selected geometrical, electronic and optical properties of compounds **1** and **2**, together with the corresponding protonated form and the radical and dicationic species, respectively, are reported in Table 2. The neutral compounds, **1** and **2**, are characterized by quite similar geometrical, electronic and optical properties. They possess small dipole moments in the ground state (μ_g = 3.49 and 3.39 D for **1** and **2**, respectively) and essentially the same structural parameters in the TTF unit. In particular, the formally double bonds of TTF, C1=C2 and C3=C4, the former being the inter-ring bond and the latter the terminal olefinic bond (see Figure S3) are close to those expected for a Csp^2=Csp^2 conjugated bond.[24] The computed electronic absorption spectra provide the low energy transitions at λ_{max} = 543 nm (**1**) and 545 nm (**2**) which compare well with the experimental values λ_{max} = 542 nm (**1**) and 532 nm (**2**) (see plots of the computed spectra for **1** and **2** in Figures S4 and S5, respectively). They correspond to $\pi_{HOMO}\rightarrow\pi^*_{LUMO}$ transitions, where HOMO and LUMO are localized on the donor (TTF) and the acceptor (dppz and BTD) moieties of the chromophores, respectively (see Figure 5 and Figure 6, left). Such ICT transitions are characterized by a significant increase of the dipole moment (μ_e = 22.05 and 16.27 D for **1** and **2**, respectively), which could account for the non-negligible experimental second order NLO response for both neutral chromophores, though largely underestimated by CP-KS calculations which provided very low hyperpolarizability projections along the dipole moment directions, $\beta_{||}$. Finite Field calculations, recently reported for analogue TTF-fused phenazine systems, provided as well low hyperpolarizability values.[10h]

An assessment of both the more probable protonation sites and the protonation degree of **1** has been performed by optimizing all the possible protonated forms and computing their relative stability, excitation energies and hyperpolarizability (see Table S1).

Four basic nitrogen sites are in fact present in compound **1**, two at the pyridyl subunits and two at the phenazine core, which may be potentially protonated by exposure to HCl vapors.

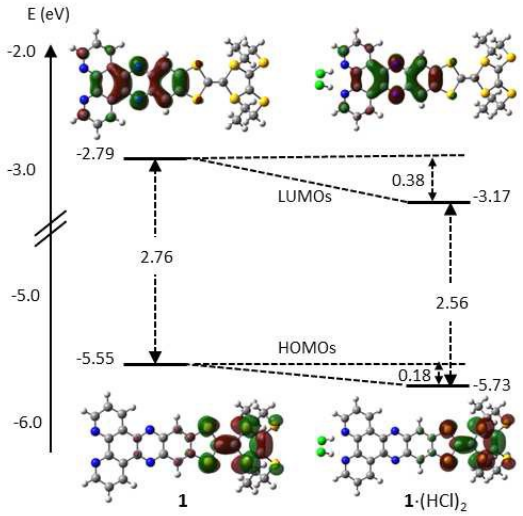

Figure 5. Frontier molecular orbitals involved in the lower energy transitions of **1** (left) and $\mathbf{1}\cdot(HCl)_2$ (right). Isosurfaces value 0.03 a.u.

The protonation degree of **1** *in vacuo* has been performed by optimizing all the possible protonated forms and computing their relative stability, excitation energies and hyperpolarizability (see Table S1), given that chloroform, used for the experimental measurements, is not expected to significantly affect the relative stability of the different protonated forms, either through polarization effects, owing to its low dielectric constant, or by specific solute-solvent interactions.

By varying the number of HCl molecules placed in proximity of the N atoms from 1 to 4, we predict that mono-, tri- and tetraprotonated species can be excluded by a direct comparison of the lowest energy absorption band centered at 600 nm to their predicated values (λ_{calc} = 569 nm for the former, λ_{calc} > 650 nm for the latter). Protonation is anticipated to occur at a pyridyl rather than a phenazine N atom due to the lower stability (by about 5 kcal/mol) of the latter species (see also ref. 24). The best agreement with the UV-vis spectrum is achieved by protonation at two N atoms of the pyridyl subunits (λ_{calc} = 589 nm), leading to the most stable diprotonated species. This result is further verified by ^{1}H NMR data. A plot of the computed absorption spectrum for $\mathbf{1}\cdot(HCl)_2$ (see Figure S4, left) highlights the good agreement with the corresponding experimental one. The molecular geometry of the $\mathbf{1}\cdot(HCl)_2$ species is not substantially modified with respect to **1**, showing essentially the same HOMO and LUMO delocalization scheme (Figure 5, right), comparable increase of the dipole moments going from the ground to the excited states and modest red-shift of the absorption band, in close agreement with the experimental spectrum (46 *vs* 59 nm, respectively). All these features account for the observed modest increase of $\mu\beta_\lambda$ going from the neutral to the protonated form, as verified by CP-KS calculations. It is

View Article Online
DOI: 10.1039/C7CP04687A

interesting to note that a simulation of the protonated $\mathbf{1}\cdot H_2^{2+}$ system, excluding the Cl^- counter anions, provides a much larger and negative $\mu\beta_\lambda$ product, at variance with the experimental result, demonstrating that in $CHCl_3$, at the concentrations used here for EFISH measurements (2×10^{-4} M), the ion pair is not dissociated as previously reported.[14]

Geometry optimization of the oxidized forms of **2** resulted in essentially planar skeletons, in spite of an expected twisted structure for $\mathbf{2}^{2+}$ (see Computational details), with significantly lengthened C1=C2 and C3=C4 bond distances, approaching the value of a Csp^2–Csp^2 conjugated bond,[26] and increased ground state dipole moments (8.46 and 14.93 D for $\mathbf{2}^{+\cdot}$ and $\mathbf{2}^{2+}$, respectively). Calculation of the UV-vis spectrum of $\mathbf{2}^{+\cdot}$ (see Figure S5 top, right), while providing high energy excitations rather blue-shifted with respect to the experimental ones, gave a lower energy $\pi_{\beta\text{-HOMO}}\rightarrow\pi^*_{\beta\text{-LUMO}}$ electronic transition at 884 nm, in close agreement with the experimental spectrum. A completely different delocalization scheme of the frontier orbitals with respect to that of the starting neutral compound was obtained in this case. The singularly occupied (β)-LUMO is in fact delocalized on the TTF moiety, *i.e.*, on the opposite side with respect to **2**. The (β)-HOMO, on the other hand, is delocalized on the whole molecule, with a slight predominance of the TTF unit (Figure 6, center). As a result, the low energy transition computed for $\mathbf{2}^{+\cdot}$ was associated with almost negligible charge-transfer character, and the dipole moment increased by about 1.5 D from the ground to the excited state.

A positive $\beta_\parallel$ was computed for $\mathbf{2}^{+\cdot}$, in contrast to the EFISH measurements that provided a negative β_0 value (Table 1). Such disagreement with the experimental finding could be explained both by resonance effect which affects the experimental value, and by the small magnitude of the $\Delta\boldsymbol{\mu}$ vector, which is responsible for the β sign according to the Oudar's two-levels model, $\beta \propto (\mu^2_{eg}\Delta\boldsymbol{\mu}/\Delta E^2_{eg})$, wherein μ_{eg} is the transition dipole moment and ΔE_{eg} the excitation energy.[25] Its orientation can in fact be perturbed by solvent and/or intrinsic effects, which could not be correctly described by the adopted computational approach, considering the notorious difficulties in treating open-shell systems.[27] It is also interesting to note that the (β)-HOMO-1 orbital, though not involved in the lowest energy transition, is placed only -0.06 eV below (β)-HOMO and is strictly localized on the BTD moiety. The relative ordering of these two levels, which could as well be influenced by subtle electronic factors, is therefore crucial in determining the CT direction associated with the lowest energy transition.

In the case of the dication, $\mathbf{2}^{2+}$, the first significant excitation was computed at 681 nm corresponding to a HOMO-1→LUMO transition, and a much weaker excitation was computed at 1401 nm, with f = 0.01, corresponding to a HOMO→LUMO transition.

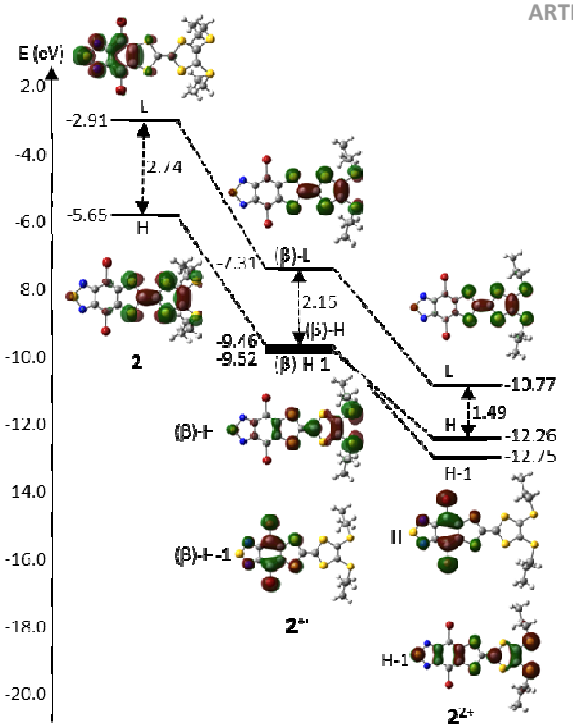

Figure 6. Energetic levels (eV) and isodensity plots of the frontier molecular orbitals of **2**, $\mathbf{2}^{+\cdot}$ and $\mathbf{2}^{2+}$ (H and L stand for HOMO and LUMO, respectively). Isosurfaces value 0.03 a.u.

Table 2. Computed Bond Lengths, Dipole Moments (μ_g and μ_e for Ground and Excited States, Respectively), Absorption Wavelengths with Associated Oscillator Strengths (in Parentheses), and Static ($\beta_{0,\parallel}$) and Dynamic (λ = 1907 nm, $\beta_\parallel$) First Hyperpolarizability Along the Dipole Moment Direction for Compounds **1**, $\mathbf{1}\cdot(HCl)_2$, **2**, $\mathbf{2}^{+\cdot}$ and $\mathbf{2}^{2+}$.[a]

Comp	C1=C2 (Å)	C3=C4 (Å)	μ_g (D)	μ_e (D)	λ (nm)	$\beta_{0,\parallel}$	$\beta_\parallel$ [b]	$\mu\beta_\parallel$ [c]
1	1.346	1.352	3.5	22.0	543 (0.30)	22.2	24.4	85
$\mathbf{1}\cdot(HCl)_2$	1.347	1.352	9.3	29.3	589 (0.30)	66.3	73.4	681
2	1.346	1.352	3.4	16.3	545 (0.21)	7.7	8.4	28
$\mathbf{2}^{+\cdot}$	1.379	1.382	8.5	9.9	884 (0.23)	89.7	139.3	1178
$\mathbf{2}^{2+}$	1.412	1.423	14.9	2.9	1401 (0.01)	-19.6	-30.1	-448

[a] $\beta_\parallel = 1/5\Sigma_i(\beta_{zij} + \beta_{jzj} + \beta_{jjz})$, the *z*-axis being aligned along the dipole moment direction. Geometries optimized at (U)PBE0/6-311++G(d,p) level of theory, absorption wavelengths and first hyperpolarizabilities computed at TD-(U)PBE0/6-311++G(d,p) and CP-(U)CAM-B3LYP/6-311++G(d,p) levels of theory, respectively. All calculations performed *in vacuo*. [b] $\beta_\parallel \times10^{-30}$ esu. [c] $\mu\beta_\parallel \times10^{-48}$ esu.

The plots of the involved frontier orbitals (Figure 6, right) reveal a completely different electronic distribution with respect to that obtained for the neutral compound. HOMO-1 is in fact delocalized on the whole molecule, HOMO is localized on the BTD unit and the LUMO is distributed on the TTF moiety. This results in a scarcely polar species in the excited state and, as a consequence, in a strong decrease of the dipole moment from the ground to the excited state (see Table 2). Though the overall appearance of the computed spectrum transition (see Figure S5, bottom) was rather far from the

View Article Online
DOI: 10.1039/C7CP04687A

measured one (a result however confirmed by using other functionals besides PBE0, such as CAM-B3LYP and M06-2X), the prediction of a negative $\Delta\mu$ and, accordingly, of a negative $\beta_{\parallel}$, is in full agreement with the experimental result.

Conclusions

An experimental and theoretical investigation on the NLO response of TTF-fused D–A systems has been carried out. Depending on the electron acceptor type, the effects on the NLO properties triggered by a pH or a redox stimulus are determined. A reversible NLO contrast (enhancement factor equal to 1.5) has been achieved by exposure of TTF-dppz (**1**) to HCl or NH_3 vapor, due to sequential protonation/deprotonation. A two-step redox modulation of the NLO efficiency has been performed on the TTF-BTD (**2**) molecule. The resulting final dication $\mathbf{2}^{2+}$ shows an increased contrast (equal to 3.7) and inversion of the sign of β_0. This inversion should be associated with a redistribution of the frontier molecular orbitals with respect to that of the starting neutral compound resulting in a scarcely polar species in the excited state, as indicated by the theoretical calculations. The latter, however, fail to predict the negative sign of β_0 of $\mathbf{2}^{+\cdot}$ probably due both to resonance contribution to the experimental value and to the almost negligible charge-transfer character of the low energy transition of $\mathbf{2}^{+\cdot}$.
These results confirm the potential and versatility of TTF-fused materials for the development of stimuli responsive organic optoelectronic materials.

Conflicts of interest

There are no conflicts of interest to declare.

Acknowledgements

The Swiss National Science Foundation and the European Commission (EC) FP7 ITN MOLESCO (Project No. 606728), are gratefully acknowledged. We deeply thank Prof. Isabelle Ledoux for fruitful discussions.

References

1 (a) *TTF Chemistry: Fundamentals and applications of Tetrathiafulvalene* (Eds: J. Yamada, T. Sugimoto), Springer, Berlin, 2004; (b) M. Bendikov, F. Wudl and D. F. Perepichka, *Chem. Rev.*, 2004, **104**, 4891; (c) N. Martín, *Chem. Commun.*, 2013, **49**, 7025; (d) Y. Geng, R. Pfattner, A. Campos, J. Hauser, V. Laukhin, J. Puigdollers, J. Veciana, M. Mas-Torrent, C. Rovira, S. Decurtins and S.-X. Liu, *Chem. Eur. J.*, 2014, **20**, 7136; (e) P. Alemany, E. Canadell, Y. Geng, J. Hauser, P. Macchi, K. Krämer, S. Decurtins, and S.-X. Liu, *Chem. Phys. Chem*., 2015, **16**, 1361.

2 (a) M. R. Bryce, A. S. Batsanov, T. Finn, T. K. Hansen, J. A. K. Howard, M. Kamenjicki, I. K. Lednev and S. A. Asher, *Chem. Commun.*, 2000, 295; (b) J. Wu, N. Dupont, S.-X. Liu, A. Neels, A. Hauser and S. Decurtins, *Chem. Asian J.*, 2009, **4**, 392; (c) J. Xiong, L. Cui, W. Liu, J. E. Beves, Y.-Y. Li, and J.-L. Zuo, *Tetrahedron Lett*., 2013, **54**, 1998.

3 (a) N. Martín, L. Sánchez and D. M. Guldi, *Chem. Commun.*, 2000, 113; (b) R. Berridge, P. J. Skabara, C. Pozo-Gonzalo, A. Kanibolotsky, J. Lohr, J. J. W. McDouall, E. J. L. McInnes, J. Wolowska, C. Winder, N. S. Sariciftci, R. W. Harrington and W. Clegg, *J. Phys. Chem. B*, 2006, **110**, 3140; (c) S. Wenger, P.-A. Bouit, Q. Chen, J. Teuscher, D. Di Censo, R. Humphry-Baker, J.-E. Moser, J. L. Delgado, N. Martín, S. M. Zakeeruddin and M. Grätzel, *J. Am. Chem. Soc.*, 2010, **132**, 5164; (d) A. Amacher, C. Yi, J. Yang, M. P. Bircher, Y. Fu, M. Cascella, M. Grätzel, S. Decurtins and S.-X. Liu, *Chem. Commun.*, 2014, **50**, 6540.

4 (a) M. Mas-Torrent and C. Rovira, *Chem. Soc. Rev.*, 2008, **37**, 827; (b) F. Otón, R. Pfattner, E. Pavlica, Y. Olivier, G. Bratina, J. Cornil, J. Puigdollers, R. Alcubilla, X. Fontrodona, M. Mas-Torrent, J. Veciana, and C. Rovira, *Cryst. Eng. Comm*., 2011, **13**, 6597; (c) R. Pfattner, E. Pavlica, M. Jaggi, S.-X. Liu, S. Decurtins, G. Bratina, J. Veciana, M. Mas-Torrent and C. Rovira, *J. Mater. Chem. C*, 2013, **1**, 3985; (d) A. Amacher, H. Luo, Z. Liu, M. Bircher, M. Cascella, J. Hauser, S. Decurtins, D. Zhang and S.-X. Liu, *RSC Adv.*, 2014, **4**, 2873; (e) Y. Geng,; R. Pfattner, A. Campos, W. Wang, O. Jeannin, J. Hauser, J. Puigdollers, S. T. Bromley, S. Decurtins, J. Veciana, C. Rovira, M. Mas-Torrent and S.-X. Liu, *Chem. Eur. J.*, 2014, **20**, 16672.

5 (a) J. Zyss, *Molecular Nonlinear Optics: Materials, Physics and Devices*, Academic Press, Boston, 1994; (b) M. G. Papadopoulos, A. J. Sadlej and J. Leszczynski, *Non-linear Optical Properties of Matter*, Springer, 2006.

6 a) B. J. Coe, *Chem. Eur. J.*, 1999, **5**, 2464; b) J. A. Delaire and K. Nakatani, *Chem. Rev.* 2000, **100**, 1817; c) I. Asselberghs, K. Clays, A. Persoons, M. D. Ward and J. McCleverty, *J. Mater. Chem.* 2004, **14**, 2831; d) V. Guerchais, L. Ordronneau and H. Le Bozec, *Coord. Chem. Rev.*, 2010, **254**, 2533; e) K. A. Green, M. P. Cifuentes, M. Samoc and M. G. Humphrey, *Coord. Chem. Rev.*, 2011, **255**, 2530; f) F. Castet, V. Rodriguez, J. L. Pozzo, L. Ducasse, A. Plaquet and B. Champagne, *Acc. Chem. Res.*, 2013, **46**, 2656; g) P. G. Lacroix, I. Malfant and C. Lepetit, *Coord. Chem. Rev.*, 2016, **308**, 381.

7 a) A. Plaquet, B. Champagne, J. Kulhánek, F. Bureš, E. Bogdan, F. Castet, L. Ducasse and V. Rodriguez, *ChemPhysChem*, 2011, **12**, 3245; b) F. Castet, B. Champagne, F. Pina and V. Rodriguez, *ChemPhysChem* 2014, **15**, 2221; c) F. Bondu, R. Hadji, G. Szalóki, O. Alévêque, L. Sanguinet, J. L. Pozzo, D. Cavagnat, T. Buffeteau and V. Rodriguez, *J. Phys. Chem. B*, 2015, **119**, 6758; d) J. Boixel, V. Guerchais, H. Le Bozec, A. Chantzis, D. Jacquemin, A. Colombo, C. Dragonetti, D. Marinotto and D. Roberto, *Chem. Commun.* 2015, **51**, 7805; e) S. van Bezouw, J. Campo, S. H. Lee, O. P. Kwon and W. Wenseleers, *J. Phys. Chem. C* 2015, **119**, 21658; f) P. Beaujean, F. Bondu, A. Plaquet, J. Garcia-Amorós, J. Cusido, F. M. Raymo, F. Castet, V. Rodriguez and B. Champagne, *J. Am. Chem. Soc.* 2016, **138**, 5052; g) K. Pielak, F. Bondu, L. Sanguinet, V. Rodriguez, B. Champagne and F. Castet, *J. Phys. Chem. C* 2017, **121**, 1851.

8 (a) R. Andreu, A. I. de Lucas, J. Garín, N. Martín, J. Orduna, L. Sánchez, and C. Seoane, *Synth. Met.,* 1997, **86**, 1817; (b) A. I. de Lucas, N. Martín, L. Sánchez, C. Seoane, R. Andreu, J. Garín, J. Orduna, R. Alcalá and B. Villacampa, *Tetrahedron,* 1998, **54**, 4655; (c) M. A. Herranz, N. Martín, L. Sánchez, J. Garín, J. Orduna, R. Alcalá, B. Villacampa and C. Sánchez, *Tetrahedron,* 1998, **54**, 11651.

9 (a) J. Garín, J. Orduna, J. I. Rupérez, R. Alcalá, B. Villacampa, C. Sánchez, N. Martín, J. L. Segura and M. González, *Tetrahedron Lett.*, 1998, **39**, 3577; (b) M. González, N. Martín, J. L. Segura, C. Seoane, J. Garín, J. Orduna, R. Alcalá, C. Sánchez and B. Villacampa, *Tetrahedron Lett.*, 1999, **40**, 8599; (c) R. Andreu, I. Malfant, P. G. Lacroix and P. Cassoux,

View Article Online
DOI: 10.1039/C7CP04687A

Synth. Met., 1999, **102**, 1575; (d) M. R. Bryce, A. Green, A. J. Moore, D. F. Perepichka, A. S. Batsanov, J. A. K. Howard, I. Ledoux-Rak, M. González, N. Martín, J. L. Segura, J. Garín, J. Orduna, R. Alcalá and B. Villacampa, *Eur. J. Org. Chem.*, 2001, 1927; (e) M. González, J. L. Segura, C. Seoane, N. Martín, J. Garín, J. Orduna, R. Alcalá, B. Villacampa, V. Hernández and J. T. López Navarrete, *J. Org. Chem.*, 2001, **66**, 8872; (f) M. Otero, M. A. Herranz, C. Seoane, N. Martín, J. Garín, J. Orduna, R. Alcalá and B. Villacampa, *Tetrahedron*, 2002, **58**, 7463; (g) J. L. Segura, and N. Martín, *Angew. Chem. Int. Ed.*, 2001, **40**, 1372 (h) J. F. Lamère, I. Malfant, A. Sournia-Saquet, P. G. Lacroix, J. M. Fabre, L. Kaboub, T. Abbaz, A.-K. Gouasmia, I. Asselberghs, and K. Clays, *Chem. Mater.*, 2007, **19**, 805.

10 (a) C.-G. Liu, W. Guan, P. Song, L.-K. Yan and Z.-M. Su, *Inorg. Chem.*, 2009, **48**, 6548; (b) L. Serrano-Andrés, A. Avramopoulos, J. Li, P. Labéguerie, D. Bégué, V. Kellö, and M. G. Papadopoulos, *J. Chem. Phys.*, 2009, **131**,134312; (c) C.-G. Liu, X.-H. Guan and Z.-M. Su, *J. Phys. Chem. C*, 2011, **115**, 6024; (d) C.-G. Liu, Z.-M. Su, X.-H. Guan and S. Muhammad, *J. Phys. Chem. C*, 2011, **115**, 23946; (e) C.-G. Liu and X.-H. Guan, *Phys. Chem. Chem. Phys.*, 2012, **14**, 5297; (f) C.-G. Liu, M.-L. Gaob and Z.-J. Wu, *RSC Adv.*, 2014, **4**, 38300; (g) C.-G. Liu, *Mol. Phys.*, 2014, **112**, 199; (h) S. Muhammad, *J. Mol. Graph. Modell.*, 2015, **59**, 14; (i) W.-Y. Wang, N.-N. Ma, L. Wang, C.-L. Zhu, X.-Y. Fang and Y.-Q. Qiu, *Dyes Pigments*, 2016, **126**, 29; (l) A. Avramopoulos, H. Reis, N. Otero, P. Karamanis, C. Pouchan, and M. G. Papadopoulos, *J. Phys. Chem. C*, 2016, **120**, 9419.

11 (a) J. J. Bergkamp, S. Decurtins and S.-X. Liu, *Chem. Soc. Rev.*, 2015, **44**, 863; (b) X. Guégano, A. L. Kanibolotsky, C. Blum, S. F. L. Mertens, S.-X. Liu, A. Neels, H. Hagemann, P. J. Skabara, S. Leutwyler, T. Wandlowski, A. Hauser and S. Decurtins, *Chem. Eur. J.*, 2009, **15**, 63.

12 (a) C. Jia, S.-X. Liu, C. Tanner, C. Leiggener, A. Neels, L. Sanguinet, E. Levillain, S. Leutwyler, A. Hauser and S. Decurtins, *Chem. Eur. J.*, 2007, **13**, 3804; (b) G. Lapadula, D. Trummer, M. P. Conley, M. Steinmann, Y.-F. Ran, S. Brasselet, Y. Guyot, O. Maury, S. Decurtins, S.-X. Liu and C. Copéret, *Chem. Mater.*, 2015, **27**, 2033.

13 F. Pop, A. Amacher, N. Avarvari, J. Ding, L. M. L. Daku, A. Hauser, M. Koch, J. Hauser, S.-X. Liu and S. Decurtins, *Chem. Eur. J.*, 2013, **19**, 2504.

14 (a) V. Alain, M. Blanchard-Desce, I. Ledoux-Rak and J. Zyss, *Chem. Commun.*, 2000, **5**, 353; (b) E. Cariati, C. Dragonetti, E. Lucenti, F. Nisic, S. Righetto, D. Roberto and E. Tordin, *Chem. Commun.*, 2014, **50**, 1608; (c) E. Cariati, C. Botta, S. G. Danelli, A. Forni, A. Giaretta, U. Giovanella, E. Lucenti, D. Marinotto, S. Righetto and R. Ugo, *Chem. Commun.*, 2014, **50**, 14225.

15 M. Ernzerhof and G. E. Scuseria, *J. Chem. Phys.*, 1999, **110**, 5029.

16 C. Adamo and V. Barone, *J. Chem. Phys.*, 1999, **110**, 6158-6170.

17 a) D. Jacquemin, E. A. Perpète, G. E. Scuseria, I. Ciofini and C. Adamo, *J. Chem. Theory Comput.*, 2008, **4**, 123; b) D. Jacquemin, V. Wathelet, E. A. Perpète and C. Adamo, *J. Chem. Theory Comput.*, 2009, **5**, 2420; c) D. Jacquemin, A. Planchat, C. Adamo, and B. Mennucci, *J. Chem. Theory Comput.*, 2012, **8**, 2359.

18 E. Runge and E. K. U. Gross, *Phys. Rev. Lett.*, 1984, **52,** 997.

19 R. E. Stratmann, G. E. Scuseria and M. J. Frisch, *J. Chem. Phys.*, 1998, **109**, 8218.

20 M. E. Casida, *J. Mol. Struct.*, (THEOCHEM) 2009, **914**, 3.

21 T. Yanai, D. Tew and N. C. Handy, *Chem. Phys. Lett.*, 2004, **393**, 51.

22 L. E. Johnson, L. R. Dalton and B. H. Robinson, *Acc. Chem. Res.*, 2014, **47**, 3258.

23 Gaussian 09, Revision D.01, Frisch, M. J. et al., Gaussian, Inc., Wallingford CT, 2013.

24 L. Kozlov and I. Goldberg, *Acta Cryst.*, 2008, **C64**, o498.

25 (a) J. L. Oudar, *J. Chem. Phys.*, 1977, **67**, 446; (b) J. L. Oudar and D. S. Chemla, *J. Chem. Phys.*, 1977, **66**, 2664.

26 F. H. Allen, O. Kennard, D. G. Watson, L. Brammer, A. Guy Orpen and R. Taylor, *J. Chem. Soc., Perkin Trans. 2*, 1987, S1.

27 T. Bally and W. T. Borden, *Rev. Comp. Chem.*, 1999, **13**, 1.